Biosensors and Bioelectronics 52 (2014) 433–437

Contents lists available at ScienceDirect

Biosensors and Bioelectronics

journal homepage: www.elsevier.com/locate/bios

A field-deployable colorimetric bioassay for the rapid and specific detection of ribosomal RNA

Janice Duy [a,*], Rosemary L Smith [a,b], Scott D Collins [a,c], Laurie B Connell [a,d,e]

[a] Graduate School of Biomedical Sciences, ESRB–LASST, University of Maine, Orono, ME 04469, USA
[b] Department of Electrical and Computer Engineering and LASST, ESRB, University of Maine, Orono, ME 04469, USA
[c] Department of Chemistry and LASST, ESRB, University of Maine, Orono, ME 04469, USA
[d] School of Marine Sciences, Hitchner Hall, University of Maine, Orono, ME 04469, USA
[e] Department of Molecular and Biomedical Sciences, University of Maine, Orono, ME 04469, USA

ARTICLE INFO

Article history:
Received 24 February 2012
Received in revised form
9 May 2012
Accepted 29 May 2012
Available online 7 June 2012

Keywords:
Peptide nucleic acid
Hybridization
rRNA
Colorimetric
Field-compatible
Biosensor

ABSTRACT

Rapid and specific on-site detection of disease-causing or toxin-producing organisms is essential to public health and safety. Many molecular recognition methods target ribosomal RNA sequences due to their specificity and abundance in the cell. In this work RNA targets were identified and quantified using a colorimetric bioassay. Peptide nucleic acid (PNA) probes were used to capture RNA targets, and a micrococcal nuclease digestion was performed to remove all non-target nucleic acids, including single base mismatches flanked by adenines or uracils. Perfectly-matched PNA–RNA hybrids remained intact and were detected using the symmetrical cyanine dye 3,3′-diethylthiadicarbocyanine iodide ($DiSC_2(5)$). Assay applicability to complex samples was demonstrated using mixtures containing RNA sequences from two related, harmful algal bloom-causing *Alexandrium* species. Target RNA was detected even in mixtures with mismatched sequences in excess of the perfect match. The fieldability of the assay was tested with a portable two-wavelength colorimeter developed to quantify the dye-indicated hybridization signal. The colorimeter sensing performance was shown to be comparable to a laboratory spectrophotometer. This quick, inexpensive and robust system has the potential to replace laborious identification schemes in field environments.

1. Introduction

Timely and accurate identification of pathogenic microorganisms in field environments is essential for health-related and environmental monitoring. Detection schemes which target ribosomal RNA (rRNA) sequences are particularly well-suited for this application because large numbers of these molecules are present in a single cell, eliminating the necessity of amplification, and are distinguishable over closely-related species (Woese, 1987). A number of existing technologies use DNA probes to capture rRNA, including whole cell hybridization, sandwich hybridization, and RT-PCR, among others (Mothershed and Whitney, 2006; O'Connor and Glynn, 2010). However, these rRNA hybridization methods are laboratory-based and generally require long turnaround times, expensive instrumentation, and technical expertise. These shortcomings have spurred the development of diagnostic systems that can be used in the field where access to specialized equipment and techniques is limited.

An improvement in the sensitivity and selectivity of nucleic acid sequence detection has been achieved by using a peptide nucleic acid (PNA) probe sequence (Xi et al., 2003; Connell et al., 2006). This synthetic DNA analog has an uncharged pseudopeptide backbone which confers superior target-binding characteristics (Egholm et al., 1992; Egholm et al., 1993) and physicochemical robustness (Demidov et al., 1994) over native nucleic acid probes. However, the structural and ionic changes induced by the PNA probe in PNA-nucleic acid heteroduplexes prevent the binding of traditional hybridization indicators such as ethidium bromide, 8-methoxypsoralen, distamycin, and DAPI (Wittung et al., 1994). As a result, visual detection of PNA hybrids has relied on covalently-labeled PNA sequences (Stender et al., 2002), which adds significantly to the cost of these probes.

The use of the cyanine dye 3,3′-diethylthiadicarbocyanine iodide ($DiSC_2(5)$) as a rapid colorimetric indicator of PNA–DNA hybridization was pioneered by the Armitage group (Smith et al., 1999). PNA–DNA duplexes, which have increased hydrophobicity from the PNA probe, serve as templates for the aggregation of the dye in the helical minor groove (Smith et al., 1999). One advantage of using this indicator with a PNA probe is that the cyanine dye does not aggregate on mixed-base DNA–DNA hybrids (Seifert et al., 1999), so that detection can be performed in samples containing non-target nucleic acids. Other indicators, such as SYBR Green I and II, PicoGreen, and RiboGreen, indiscriminately bind to either double- or single-stranded nucleic acids, making target quantitation difficult in a mixture.

* Corresponding author. Tel.: +1 207 581 4298; fax: +1 207 581 2801.
E-mail address: janice.duy@umit.maine.edu (J. Duy).

0956-5663/$ - see front matter © 2013 Elsevier B.V. All rights reserved.
http://dx.doi.org/10.1016/j.bios.2012.05.039

The absorbance spectrum of $DiSC_2(5)$ in aqueous solution has characteristic peaks at 650 nm and 580 nm, corresponding to the dye monomer and dimer forms, respectively (West and Pearce, 1965), producing a blue solution color. Aggregation of the dye in PNA–DNA duplexes results in the blue-shifting of the $DiSC_2(5)$ absorbance peak from 650 nm to 540 nm and in an immediate solution color change from blue to purple. The simplicity and speed of this method have since been applied to the detection of PNA–DNA hybrids in various genetic screening applications (Wilhelmsson et al., 2002; Komiyama et al., 2003; Sforza et al., 2005; Tedeschi et al., 2007).

In this paper, the successful application of the $DiSC_2(5)$ colorimetric method to detect PNA–RNA hybrids is reported. This method is being developed for use in the on-site identification of pathogenic organisms without the need for sample amplification, expensive reagents and equipment, or highly trained personnel. When PNA–RNA duplexes form in the presence of ($DiSC_2(5)$) (Duy et al., 2011), the solution color immediately changes from blue (without target RNA) to purple (with target). Following hybridization, a short incubation with the relatively non-specific micrococcal nuclease enabled the detection of point mutations within minutes, without affecting the perfectly-matched hybrid. To demonstrate the feasibility of using this method in non-laboratory settings, an inexpensive two-wavelength colorimeter was designed specifically for this assay and assembled from commercially available components. The handheld instrument was tested against a laboratory spectrophotometer and was verified to be a portable alternative to the benchtop machine.

The algal *Alexandrium tamarense/fundyense/catanella* species complex was chosen as the model organism in this study. These dinoflagellates are present in coastal waters globally (Van Dolah, 2000), and produce neurotoxins that can cause paralytic shellfish poisoning (PSP). Hence, real-time monitoring of these organisms is critical for the prevention of beach closures and animal casualties. In addition, harmful and benign species are nearly impossible to differentiate visually, so nucleic acid-based identification is required. The target sequence used in this study is located in the D1–D2 hypervariable region of the 28S rRNA and has been verified as specific and suitable for hybridization assays (Anderson et al., 1999, 2005).

2. Materials and methods

2.1. Oligonucleotides and reagents

A PNA sequence complementary to the large-subunit ribosomal RNA of the North American *Alexandrium tamarense/fundyense/catanella* ribotype, NA1 (Anderson et al., 1999) was purchased from PNA Bio, Inc. (Thousand Oaks, CA, USA). RNA oligonucleotides were purchased from Integrated DNA Technologies (Coralville, IA, USA). The probe and target sequences are given in Table 1. The PNA probes were resuspended in molecular biology-grade water, while RNA stock solutions were made in the RNA Storage Solution (1 mM sodium citrate, pH 6.4) from Ambion (Austin, TX, USA). Micrococcal nuclease was purchased from New England BioLabs (Ipswich, MA, USA). The dye 3,3′-diethylthiadicarbocyanine iodide (dye content 98%) was purchased from Sigma Aldrich (St. Louis, MO, USA) and 2 mM stock solutions were prepared in methanol.

2.2. PNA–RNA hybridization and specificity experiments

Nucleic acid hybridization was performed in 0.2 mL DNase- and RNase-free thin-walled polypropylene PCR tubes (Molecular BioProducts, San Diego, CA, USA) in a total volume of 20 μL. Note that all quantities given refer to final concentrations in solution. PNA probes (1 μM) and RNA oligonucleotides (varying concentrations) were mixed in hybridization buffer (50 mM Tris–HCl, 5 mM $CaCl_2$, pH 7.9). The mixture was kept at 25 °C for 5 min in a dry heat block, after which micrococcal nuclease (100 Kunitz units) was added and the solution was incubated for a further 5 mins. $DiSC_2(5)$ in methanol (10 μM) was then mixed in, and absorbance spectra were recorded immediately after dye addition. Spectrophotometer readings were made using 2 μL of sample with a NanoDrop ND-1000 (Thermo Fisher Scientific Inc., Waltham, MA, USA).

In order to construct a concentration response curve for the target RNA, nucleic acid hybridization was performed as described above, with *A. tamarense* RNA diluted to final concentrations of 100, 250, 500, 750, and 1000 nM. Assay specificity for *A. tamarense* in the presence of competing *A. ostenfeldii* sequences was assessed with samples containing both target and non-target *Alexandrium* RNA. The target *A. tamarense* RNA concentration was varied (100, 250, 500, 750, and 900 nM), and *A. ostenfeldii* (non-target) RNA was added to bring the total RNA concentration of each sample to 1000 nM; for instance, 900 nM *A. ostenfeldii* RNA was added to the 100 nM *A. tamarense* concentration.

2.3. Handheld colorimeter design

A prototype two-wavelength colorimeter was assembled primarily from off-the-shelf parts. LED light sources were obtained from Vishay Semiconductors (Malvern, PA) and were selected to encompass the dye monomer (red, Vishay TLDR5800, λ_{peak}=652 nm) and dye aggregate (green, Vishay TLHP5800, λ_{peak}=556 nm) wavelengths. A high-output-current, dual-channel 10-bit programmable digital-to-analog converter (MAX5550, Maxim, Sunnyvale, CA, USA) was used as a constant-current source for the LEDs. The photodetector chosen for this system was a programmable light-to-frequency converter (TSL230BR-LF, TAOS, Inc., Plano, TX). User input and display were handled with a

Table 1
Oligonucleotide sequences used in this study. Mismatches in the RNA base sequences are in bold and underlined.

Oligonucleotide	Base sequence	Mismatch location
	N-terminus to C-terminus for PNA, 5′ to 3 for RNA	*Flanking RNA bases*
PNA probe	EE–GTG CAA CAC TCC CAC C–EE*	–
A. tamarense target region	GGU GGG AGU GUU GCA C	None
A. ostenfeldii target region	GGU G**A**G A**U**U GUU GC**G U**	Multiple bases
C–A mismatch	GGU GGG A**A**U GUU GCA C	–
C–C mismatch	GGU GGG A**C**U GUU GCA C	A and U
C–U mismatch	GGU GGG A**U**U GUU GCA C	–
A–A mismatch	GGU GGG AG**A** GUU GCA C	–
A–C mismatch	GGU GGG AG**C** GUU GCA C	G and G
A–G mismatch	GGU GGG AG**G** GUU GCA C	–

* E moieties are solubility enhancers (Gildea et al. 1998).

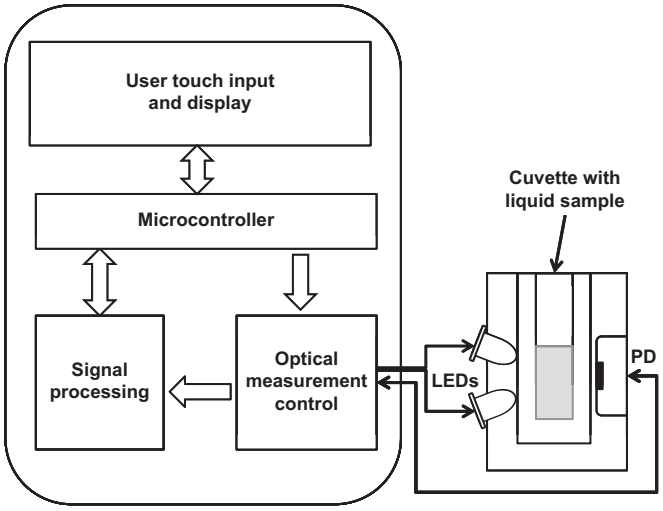

Fig. 1. Colorimeter block diagram. A functional block diagram of the colorimeter is shown. A microcontroller unit is used to run a touchscreen display and optical measurement components. A simplified drawing of the cuvette holder (side view) is included, with the positions of the LEDs (light emitting diodes) and PD (photodetector) relative to the liquid sample illustrated.

3.2″ TFT LCD module (ITDB02-3.2S, ITead Studio, Shenzen, China). For side-by-side instrument evaluation, 1-cm pathlength ultra-micro cuvettes (BrandTech Scientific, Inc., Essex, CT, USA) were used to fit both the colorimeter and a Beckman Coulter DU-640 benchtop spectrophotometer (Brea, CA, USA). A cuvette holder with integrated positioning slots for the LEDs and photodetector was designed and sent out for 3D printing (Shapeways, New York, NY, USA). An Arduino Mega 2560 was used to control all devices, and for data collection and signal processing. The colorimeter block diagram is shown in Fig. 1.

2.4. Colorimeter comparison with benchtop spectrophotometer

PNA probes (1 μM) and RNA (varying concentrations) were mixed in hybridization buffer and incubated for 5 min at 25 °C. Micrococcal nuclease (100 Kunitz units) and $DiSC_2(5)$ dye (10 μM) were added as above. The reaction volume of each sample was 200 μL. Absorbance values from 220 to 750 nm were collected using the Beckman Coulter DU-640 spectrophotometer.

For colorimeter testing, the photodetector was set to 10 × sensitivity and 2 × frequency scaling (TAOS Inc. 2006). The green LED was driven with a forward current, $I_F = 25$ mA. For instrument setup (software-controlled), the frequency output of the green LED through a blanking solution was recorded, and the forward current for the red LED was adjusted to produce the same response (typically $I_F \approx 1$ mA).

For sample reading, each LED was powered for 1 s and the photodetector output was recorded using pulse accumulation for that duration. An off time of 20 ms was introduced before the next LED was turned on to allow the photodetector signal to return to zero. Output values displayed to the user reflect two successive reads that are within 0.1% of each other. Each liquid sample was read three times consecutively to determine instrument reproducibility.

2.5. Data collection and analysis

Absorbance data from the spectrophotometer were used directly to obtain the hybridization signal, by taking the ratio of the absorbance peak magnitudes for the dye aggregate ($\lambda = 540$ nm) and monomer ($\lambda = 650$ nm):

$$H = \frac{A_{\text{aggregate}}}{A_{\text{monomer}}} \approx \frac{A_{540}}{A_{650}} \quad (1)$$

For colorimeter-based measurements, the "blank" output frequency, I_{blank}, of each LED was recorded. The absorbance of each sample was then calculated as

$$A_{\text{LED}} = -\ln\left(\frac{I_{\text{sample}}}{I_{\text{blank}}}\right) \quad (2)$$

The colorimeter hybridization signal, taken from the calculated absorbance values given in Eq. 2, was defined as

$$H = \frac{A_{\text{green}}}{A_{\text{red}}} \quad (3)$$

Data analysis was performed using OriginPro 8.6 (OriginLab Corp., Northampton, MA, USA).

3. Results and discussion

3.1. Dye indication of PNA–RNA hybridization

The dye $DiSC_2(5)$ has characteristic absorption peaks at 650 nm and 580 nm in hybridization buffer. When added to a solution containing the PNA probe alone, the positions of the dye peaks are unaltered (Fig. 2, solid line). However, when added to a solution containing PNA–RNA hybrids, a new absorption peak at ~540 nm is observed in the dye spectrum (dashed line). This shift in peak absorbance (~110 nm) is immediately visible as a color change in the solution from blue (PNA probe only) to purple (PNA–RNA hybrid) (Fig. 2, insets). This new peak is attributed to the development of higher-order dye aggregates forming in the minor groove of PNA–RNA hybrids. In PNA–DNA hybrids, $DiSC_2(5)$ aggregation is the result of cooperative binding of face-to-face dye molecules (Smith et al., 1999). While slight conformational differences in the double-helical structures of PNA–DNA and PNA–RNA hybrids exist (Eriksson and Nielsen, 1996), the position of the induced absorbance peak suggests that the mechanism of $DiSC_2(5)$ aggregation is the same for both types of hybrids (Hannah and Armitage, 2004; Hannah et al.,

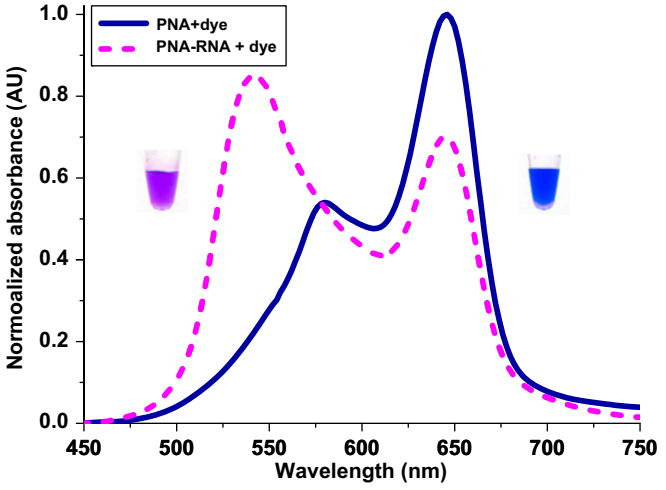

Fig. 2. Optical characteristics of indicator dye in the presence of PNA and PNA–RNA hybrids. The cyanine dye $DiSC_2(5)$ in the presence of PNA alone has characteristic peaks at 650 nm and 580 nm (solid line) and produces a blue solution. PNA–RNA hybrids induce the formation of a blue-shifted peak at ~540 nm in the dye spectrum, with a concomitant decrease in the 650 nm peak (dashed line), and the solution changes color to purple. PNA and RNA concentrations used were 1 μM, while $DiSC_2(5)$ concentration was 10 μM. Absorbance values were taken at 25 °C with a Beckman Coulter DU-640 spectrophotometer, 1 cm pathlength.

2005; Tomlinson et al., 2006). Since the dye aggregate peak at 540 nm grows at the expense of the monomer peak at 650 nm, a "hybridization signal" can be defined as the ratio of these two values (Eq. 1).

One advantage of this method is the rapid response associated with using a PNA probe. While PNA–RNA hybridization was allowed to proceed for five minutes for protocol reproducibility, hybridization was complete within seconds (Rose, 1993 and unpublished data). In contrast, most nucleic acid-based detection schemes require much longer incubation periods (Mothershed and Whitney, 2006; O'Connor and Glynn, 2010).

3.2. Single-base mismatch discrimination of A. tamarense-based RNA sequences

The ability of the assay to recognize point mutations in RNA was evaluated by constructing artificial mismatches in the center of the target sequence (Table 1). The hybridization signal from perfectly-matched hybrids (Fig. 3, "PM") was unaffected by micrococcal nuclease digestion. No mismatches were resolved without the addition of nuclease (Fig. 3, unshaded bars), but point mutations between adenines and uracils could be reduced to background levels after nuclease treatment. The C(PNA)-C(RNA) mismatch was an exception, and produced a signal only slightly above background. Mismatches flanked by guanines, however, could not be completely digested away in the experiment time-frame of 5 min (Fig. 3, shaded bars). These findings are consistent with prior work on micrococcal nuclease: the enzyme shows a marked preference for digesting AT-rich regions, and its action is much reduced when confronted with guanines and cytosines (von Hippel and Felsenfeld, 1964; Dingwall et al., 1981; Hörz and Altenburger, 1981; Drew, 1984). It should also be noted that the A(PNA)-N(RNA) mismatches have been reported as some of the least destabilizing types to a PNA–RNA duplex (Jensen et al., 1997). These factors should be considered when using this method to identify point mutations, especially since the binding characteristics of each probe sequence must be empirically determined (Pozhitkov et al., 2006).

Other investigators have used the single-strand-specific endonuclease S1 to digest all types of single-nucleotide mismatches in PNA–DNA hybrids (Komiyama et al., 2003; Ye et al., 2007), but this approach requires additional steps such as buffer change/salt addition, a lengthy incubation time, and a stop solution. Furthermore, the applicability of S1 nuclease is limited to unstructured nucleic acid sequences, which precludes its use with genomic DNA or RNA (Ren et al., 2004). Micrococcal nuclease completely digests single- and double-stranded nucleic acids without degrading PNA–RNA hybrids. Hence, target sequences in environmental samples do not need to be pre-hybridized or amplified, as the nuclease will remove non-target DNA and RNA from the mixture.

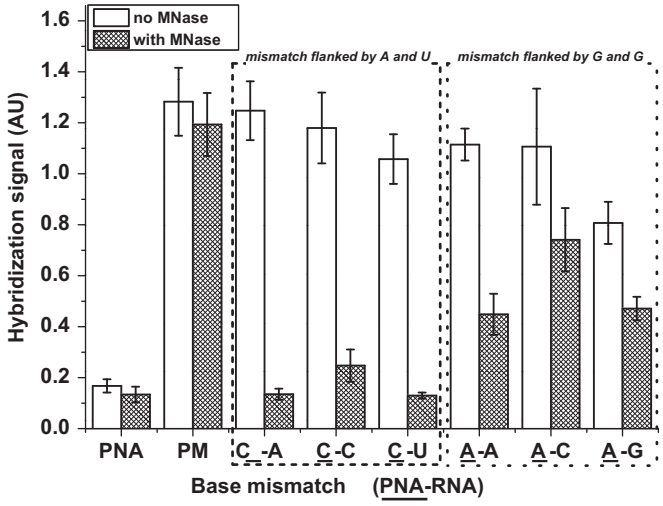

Fig. 3. Effect of micrococcal nuclease on the digestion of single-base mismatches. Perfectly-matched and single-base mismatched RNA sequences showed high hybridization signals to the PNA probe (light bars). The effect of micrococcal nuclease on these hybrids is denoted by the shaded bars. Point mutations sandwiched by adenines and uracils (C–N base mismatches, inside dashed box) were successfully differentiated from the perfect match. Guanine-flanked mismatches (A–N mismatches, inside dotted box) showed reduced hybridization signals. PM indicates the perfectly-matched PNA–RNA duplex, while base mismatches are given by N(PNA)–N(RNA). Nucleic acid concentrations used were 1 μM, while $DiSC_2(5)$ concentration was 10 μM. Absorbance values were taken at 25 °C with a NanoDrop ND-1000 spectrophotometer.

3.3. RNA concentration dependence and discrimination against A. ostenfeldii RNA

The utility of this method in quantifying the amount of target RNA present, even in mixtures with similar, non-target sequences, is shown in Fig. 4. The hybridization signal A_{540}/A_{650} was used to construct concentration curves for *A. tamarense* RNA alone, and for the same RNA mixed with *A. ostenfeldii* sequences. Without nuclease digestion, the signals from the mixed samples were uniformly high (hollow circles), as the *A. ostenfeldii* RNA sequence has only four base mismatches to the probe (Table 1), and the hybridization was performed at room temperature (25 °C). Nevertheless, nuclease treatment of the mixed-RNA samples (filled circles) yielded hybridization signals that were virtually identical to those from *A. tamarense* RNA only (triangles). RNA mixtures containing 250 nM and 500 nM of the target sequence produced lower hybridization signals than the target-only samples. This is likely due to the low hybridization temperature; presumably the large numbers of *A. ostenfeldii* RNA sequences competitively bound the PNA probes. In that case, the mismatched RNA, as well as unbound target strands, would be digested by the nuclease.

3.4. Comparison of colorimeter and spectrophotometer response

Samples of *A. tamarense* RNA at concentrations of 100, 250, 500, 750, and 1000 nM were prepared as described in Section 2.2.

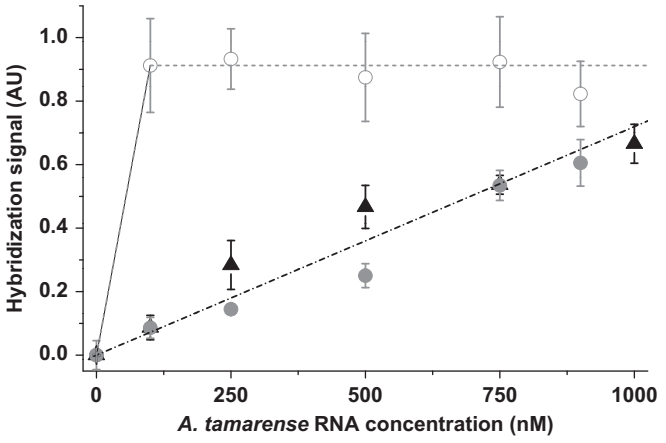

Fig. 4. Quantitative detection of *A. tamarense* RNA in mixtures with *A. ostenfeldii* RNA. A concentration curve with target RNA only (triangles) was constructed. The same concentrations of target RNA were mixed with interfering non-target RNA, allowed to hybridize to the PNA probe, and were treated (filled circles) or not treated (hollow circles) with micrococcal nuclease. The plotted lines are intended to guide the eye. The probe concentration used was 1 μM, and the dye concentration was 10 μM. Absorbance values were taken at 25 °C with a NanoDrop ND-1000 spectrophotometer.

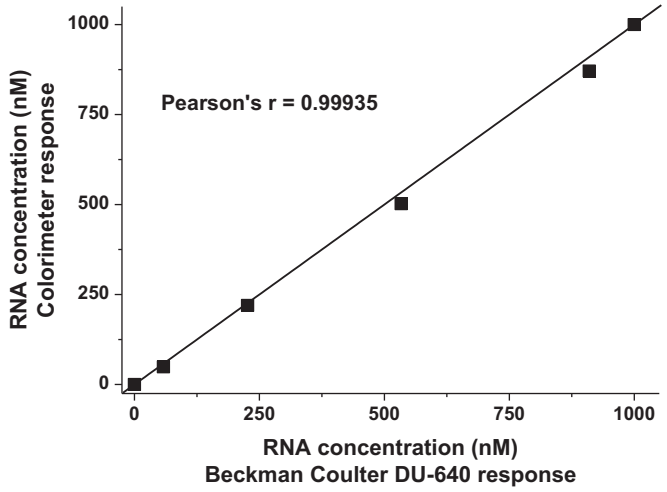

Fig. 5. Comparison of colorimeter performance to benchtop spectrophotometer. The hybridization signals obtained from the colorimeter and from a Beckman Coulter DU-640 spectrophotometer (see text for equations) were compared on a scatter plot, with a line drawn through $r=1$. The correlation between the signals obtained, at a significance level of 0.05, is $r=0.99935$. Each point represents three independent samples at the RNA concentration tested.

The hybridization signal, *H*, for each sample was measured with the prototype colorimeter and with the Beckman Coulter DU-640, using identical samples. The normalized concentration-dependent hybridization response obtained with the colorimeter plotted against that obtained with the Beckman Coulter DU-640 is shown in Fig. 5. Each point represents the average of three independent samples at the given concentration.

A Pearson's correlational analysis was performed on the two sets of data. At a significance level of $p=0.05$, the correlation coefficient $r=0.99935$: the colorimeter response is virtually identical to that of the spectrophotometer for the same samples. This indicates that the inexpensive and portable colorimeter can replace a benchtop instrument for out-of-laboratory assays.

4. Conclusion

This paper reports the first demonstration of using the cyanine dye $DiSC_2(5)$ to detect PNA–RNA hybrids in a rapid and highly specific colorimetric assay. Peptide nucleic acid (PNA) probes targeted to the toxigenic North American *Alexandrium* dinoflagellate species were used to capture complementary RNA sequences. PNA hybridization to RNA targets was almost instantaneous, and a short digestion with micrococcal nuclease eliminated all other non-target nucleic acids, including single nucleotide mismatches sandwiched by adenines or uracils. PNA–RNA duplexes were indicated by the color change (from blue to purple) of the symmetrical cyanine dye 3,3′-diethylthiadicarbocyanine iodide ($DiSC_2(5)$). This color change was due to the formation of a blue-shifted dye aggregate absorbance peak at the expense of the original dye monomer peak, enabling the amount of target RNA in the sample to be quantified by the ratio of these absorbance values. Preliminary validation of the applicability of the assay to complex samples was carried out with mixtures containing both *A. tamarense* (target) and *A. ostenfeldii* (non-target) RNA oligonucleotides. *A. tamarense* RNA could be detected even in the presence of excess *A. ostenfeldii* sequences, indicating the suitability of this method in detecting unamplified targets in environmental samples.

To validate the field-compatibility of the assay, a handheld colorimeter was designed to capture absorbance information at the dye peak wavelengths. A prototype instrument was constructed using commercially available parts and used for testing. Hybridization signals obtained from this colorimeter were found to be equivalent to those from a laboratory spectrophotometer over a range of target concentrations. Hence, this biodetection system holds great promise for the near-real-time identification of target organisms in environmental samples, without the need for costly equipment or trained operators.

Acknowledgments

The authors would like to thank Corey Hirn, Dr. Paul Millard, Prof. Don Hummels, Dr. Nuri Emanetoglu and Justin Millis for their assistance. Funding for this work was provided by the NOAA Center for Sponsored Coastal Ocean Research (CSCOR) MERHAB Program (nos. NA11NOS4780026 and NA05NOS4781232), the USDA Biosecurity (no. 2006-55605-16654) and NSF-CBET, (no. 0854020).

References

Anderson, D., Kulis, D., Keafer, B., Gribble, K., Marin, R., Scholin, C., 2005. Deep Sea Research Part II: Topical Studies in Oceanography 52 (19–21), 2467–2490.
Anderson, D.M., Kulis, D.M., Keafer, B.A., Berdalet, E., 1999. Journal of Phycology 35 (4), 870–883.
Connell, L.B., Ray, J., Litaker, W., Tester, P., 2006. African Journal of Marine Science 28 (2), 237–239.
Demidov, V.V., Potaman, V.N., Frank-Kamenetskil, M.D., Egholm, M., Buchard, O., Sönnichsen, S.H., Nielsen, P.E., 1994. Biochemical Pharmacology 48 (6), 1310–1313.
Dingwall, C., Lomonossoff, G.P., Laskey, R.A., 1981. Nucleic Acids Research 9 (12), 2659–2673.
Drew, H.R., 1984. Journal of Molecular Biology 176, 535–557.
Duy, J., Smith, R.L., Collins, S.D., Connell, L.B., 2011. OCEANS 2011, 1–5.
Egholm, M., Buchardt, O., Christensen, L., Behrens, C., Freier, S.M., Driver, D.A., Berg, R.H., Kim, S.K., Nordén, B., Nielsen, P.E., 1993. Nature 365, 566–568.
Egholm, M., Buchardt, O., Nielsen, P.E., Berg, R.H., 1992. Journal of the American Chemical Society 114, 1895–1897.
Eriksson, M., Nielsen, P.E., 1996. Quarterly Reviews of Biophysics 29 (4), 369–394.
Gildea, B.D., Casey, S., MacNeill, J., Perry-O'Keefe, H., Sørensen, D., Coull, J.M., 1998. Tetrahedron Letters 39 (1), 7255–7258.
Hannah, K.C., Armitage, B.A., 2004. Accounts of Chemical Research 37, 845–853.
Hannah, K.C., Gil, R.R., Armitage, B.A., 2005. Biochemistry 44 (48), 15924–15929.
Hörz, W., Altenburger, W., 1981. Nucleic Acids Research 9 (12), 2643–2658.
T.A.O.S. Inc., 2006. TSL230R-LF, TSL230AR-LF, TSL230BR-LF. Plano, TX, pp. 1–8.
Jensen, K.K., Ørum, H., Nielsen, P.E., Nordén, B., 1997. Biochemistry 36, 5072–5077.
Komiyama, M., Ye, S., Liang, X., Yamamoto, Y., Tomita, T., Zhou, J.-M., Aburatani, H., 2003. Journal of the American Chemical Society 125, 3758–3762.
Mothershed, E.A., Whitney, A.M., 2006. Clinica Chimica Acta 363, 206–220.
O'Connor, L., Glynn, B., 2010. Expert Review of Medical Devices 7 (4), 529–539.
Pozhitkov, A., Noble, P.A., Domazet-Loso, T., Nolte, A.W., Sonnenberg, R., Staehler, P., Beier, M., Tautz, D., 2006. Nucleic Acids Research 34 (9), e66.
Ren, B., Zhou, J.-M., Komiyama, M., 2004. Nucleic Acids Research 32 (4), e42.
Rose, D.J., 1993. Analytical Chemistry 65 (24), 3545–3549.
Seifert, J.L., Connor, R.E., Kushon, S.A., Wang, M., Armitage, B.A., 1999. Journal of the American Chemical Society 121, 2987–2995.
Sforza, S., Scaravelli, E., Corradini, R., Marchelli, R., 2005. Chirality 17 (9), 515–521.
Smith, J.O., Olson, D.A., Armitage, B.A., 1999. Journal of the American Chemical Society 121 (12), 2686–2695.
Stender, H., Fiandaca, M.J., Hyldig-Nielsen, J.J., Coull, J., 2002. Journal of Microbiological Methods 48 (1), 1–17.
Tedeschi, T., Sforza, S., Ye, S., Corradini, R., Dossena, A., Komiyama, M., Marchelli, R., 2007. Journal of Biochemical and Biophysical Methods 70 (5), 735–741.
Tomlinson, A., Frezza, B., Kofke, M., Wang, M., Armitage, B.A., Yaron, D., 2006. Chemical Physics 325 (1), 36–47.
Van Dolah, F.M., 2000. Environmental Health Perspectives 108 (Suppl. 1), 133–141.
von Hippel, P.H., Felsenfeld, G., 1964. Biochemistry 3 (1), 27–39.
West, W., Pearce, S., 1965. Journal of Physical Chemistry 69 (6), 1894–1903.
Wilhelmsson, L.M., Nordén, B., Mukherjee, K., Dulay, M.T., Zare, R.N., 2002. Nucleic Acids Research 30, e3.
Wittung, P., Kim, S.K., Buchard, O., Nielsen, P.E., Nordén, B., 1994. Nucleic Acids Research 22 (24), 5371–5377.
Woese, C.R., 1987. Microbiological Reviews 51 (2), 221–271.
Xi, C., Balberg, M., Boppart, S.A., Raskin, L., 2003. Applied and Environmental Microbiology 69 (9), 5673–5678.
Ye, S., Miyajima, Y., Ohnishi, T., Yamamoto, Y., Komiyama, M., 2007. Analytical Biochemistry 363 (2), 300–302.